NUMERICAL STUDY OF TRIPLE DIFFUSIVE MHD RADIATIVE CASSON FLUID FLOW OVER A VERTICAL WALL WITH CHEMICAL REACTION & HEAT SOURCE/SINK IMPACTS

Atiya Ali[1] , Ruchika Mehta[1*], Renu Sharma[2] and Sushila[3]
[1,1*] Department of Mathematics and Statistics,
Manipal University Jaipur,
Jaipur-303007, Rajasthan, India
[2]Department of Physics, JECRC University,
Jaipur-303905, Rajasthan, India
[3]Department of Physics, Vivekananda Global University,
Jaipur-303012, Rajasthan,India
[1*]ruchika.mehta1981@gmail.com

Abstract

The present study focuses on the MHD Radiative Casson fluid flow with the effect of triple diffusivity over a vertical porous wall along with convective boundary conditions. The governing equations for detecting the nature of the fluid under the influence of solutal diffusivity and thermal conductivity in triple diffusive boundary layer flow are derived. Non-linear partial differential equations are reduced to ordinary differential equations via similarity transformation. The BVP4C method in MATLAB software is then used to solve them. The outcomes of several physical dimensionless parameters like permeability, convective parameter, buoyancy ratio parameter, Casson parameter and chemical reaction parameter with source/sink impacts established by graphics. Also, the impression of the local skin friction coefficient, Nusselt number, and local Sherwood number are presented through the tables.
Key words: MHD; Vertical wall; Casson fluid; Mixed Convection; Buoyancy; Triple diffusive; Brownian motion.

Table 1: Symbols List:

B_0	Magnetic induction	π	deformation rate Multiple factors
Sc_1	Schmidt parameter for concentration profile 1	π_c	Critical value of πfounded on non-Newtonian model
Sc_2	Schmidt parameter for concentration profile 2	e_{ij}	$(i,j)^{th}$ deformation rate factor
C_n	Concentration profile n,(n=1,2)	Nr	Radiation parameter
$C_{n\infty}$	Ambient concentration n,(n=1,2) as y tends to infinity	Ec	Eckert number
C_{nw}	reference concentration profile n,(n=1,2)	M	Magnetic field parameter
C_p	Specific heat capacity	Pr	Prandtl number
D_{B1}	Brownian diffusion coefficient for concentration profile 1	Re_x	Local Reynolds number
D_{B2}	Brownian diffusion coefficient for concentration profile 2	G_T	local temperature Grashof number
D_m	Mass diffusivity	G_{C1}	local Grashof number for concentration profile 1
K	parameter of Porous media	G_{C2}	local Grashof number for concentration profile 2
k	the porous medium Permeability	R_0	Chemical reaction coefficient
Sh_{x1}	Local Sherwood number for concentration profile 1	R_1	Chemical reaction parameter for concentration profile 1
Sh_{x2}	Local Sherwood number for concentration profile 2	R_2	Chemical reaction parameter for concentration profile 2
n	viscosity factor (Constant)	T	Temperature of the nanofluid within the boundary layer
Q_0	The heat Source/sink coefficient(dimensional)	T_W	Reference temperature
q	Radiative heat flux	T_∞	Ambient fluid Temperature
N_1	The Buoyancy force parameter for concentration profile 2	T_f	constant fluid temperature
N_2	The Buoyancy force parameter for concentration profile 2	Nu_x	Local Nusselt number
C_{fx}	The Skin friction coefficient	h_f	variable heat transfer

	Greek Symbols
θ	Dimensionless temperature
ϕ_n	Dimensionless concentration(n-1,2)
ν	viscosity Kinematic coefficient
α	Thermal Diffusivity
β	parameter of Casson Fluid
σ	The electrical conductivity
λ	The heat source/sink parameter
λ_1	Mixed convection parameter
η	Similarity variable
τ	Heat capacity ratio
τ_w	wall shear stress of the fluid
μ_B	Non-Newtonian plastic dynamic viscosity

u, v	components of Velocity along x- and y- directions, respectively
u_w	Reference velocity
$x.y$	Cartesian coordinates along and normal to the plate, respectively
Subscripts	
w	Surface conditions
∞	Conditions far away from the surfaces
Superscripts	
$'$	Differentiation with respect to η

1 Introduction

The non-Newtonian fluid is an essential part of our daily lives and is utilized in various applications. These fluids are used as drag-reducing agents, in printing technology, and as damping and braking devices. They are also used in personal protective equipment and food products. These versatile fluids have many uses and are an essential part of modern technology. In the Engineering sector, Industries and the Research area use different applications for studying mass and heat transfer known in various theoretical and practical aspects. Triple diffusive magnetohydrodynamic (MHD) fluid flow involves the study of fluid motion that includes three distinct types of diffusion processes: thermal diffusion, mass diffusion, and magnetic diffusion. This type of flow is encountered in various physical systems and finds applications in astrophysics, geophysics, and engineering. In the case of the study of anomalies in fatty acid, uses of convection of triple diffusive observed in the modelling of medical airing tools, triglycerides and surrounding several components such as saturated fat (high-density lipoproteins, low-density-Cholesterol lipoproteins), which hold different diffusivities. Many industries, technical applications and different sectors depend on MHD fluxes and MHD generators. Devi, & Devi, (2) conducted a numerical parametric study to compare the heat transfer characteristics of nano-fluid and hybrid nano-fluid. Through these observations, they found that the rate of heat transfer of hybrid nano-fluid (Cu–Al2O3/water) is higher than that of nano-fluid (Cu/water) when a magnetic field is present. Gireesha, B.J. et al. (4) studied heat and mass transfer in a three-dimensional, double-diffusive, hydromagnetic boundary layer flow of an electrically conducted Casson nano-fluid over a stretched surface. The researchers conducted this study to take into account a variety of factors to define convective boundaries, including unsynchronized thermal radiation, electromagnetic fields, buoyancy forces, thermophoresis, and Brownian motion. Hayat, T. et al. (7) explained the study of the effects of Soret and Dufour on the magnetohydrodynamic three-dimensional 3D flow of second-grade fluid in the existence of heat radiation and effects from Soret and Dufour. The second-grade fluid is taken to be electrically conductive by means of a uniform magnetic field. Isa, et al.(9) illustrated how the exponentially permeable fabric affects the Mixed convection magnetohydrodynamic (MHD) boundary layer flow for Casson fluid. Jena, S. et al.(13) noticed the MHD viscoelastic fluid flow subject to variable magnetic field implanted in a porous medium in the existence of chemical reaction and heat source or sink with soret and Dofour effect over a porous vertical stretching sheet. Patil, et al.(25) investigated numerically on steady boundary layer flow with triple diffusive and mixed convection past a vertical plate moving corresponding to the free stream in the upward direction. Patil, et al.(25) considered solutal components like sodium chloride and sucrose which are added to the flow stream from below with various concentration levels and investigated the thermal and species concentration fields. Raghunatha, et al.(27) investigated the weakly non-linear constancy of the convection of triple diffusive in a Maxwell fluid-saturated porous layer and found that depending on the alternative of the physical parameters the bifurcating

oscillatory solution is either supercritical or subcritical. In terms of time and area-averaged Nusselt numbers Heat and mass transfers are predictable. Manjappa, et al. (21) examined the impact of non-linear triple diffusive thermal radiation on the convective boundary layer flow of Casson nano-fluid along a flat plate. The free convection of triple diffusive in triangular, square and trapezoidal permeable chambers under an effect of interior volumetric heat production was examined by Khan, et al.(14). Here the chambers with the peak surface and pedestal surfaces are supposed to be adiabatic and impenetrable. Khan, et al.(15) analyzed the entropy for triple diffusive flow and due to various effects, they found that as compared to opposing flows the assisting flows entropy generation rates are higher. Simultaneously, these entropy generation rates are reduced with some other effect. Lund, et al.(19) examined numerically a study of magnetohydrodynamic (MHD) micro polar fluid flow in the presence of joule heating effect and viscous dissipation effects on a shrinking surface. Nawaz, and Awais, (23) discussed double diffusion of nanoparticles and solute presuming using adapting finite element method for the numerical effects of diffusion thermo and thermal diffusion. Rao, et al.(29) analyzed Dufour and thermophoresis effects in magnetohydrodynamic (MHD) three-dimensional fluid motion of Newtonian and non-Newtonian and calculated the mass & heat transfer above a stretching surface with Brownian motion. Umavathi, et al.(34) explored that when heat is exchanged from the external fluid with the plates, the flow does not depend on time on triple diffusive convection in a vertical channel. Farooq, et al.(3) experimented with the essential quantities modified in the streamwise direction in the Darcy-Forchheimer-Brinkman framework. Therefore, in non-Darcy porous media, the Casson nano-fluid steady flow over a flat plate is installed and developed non-similar boundary layer model for forced convection. Parvin, et al.(24) studied the numerical solutions of magnetohydrodynamics (MHD) casson fluid flow which considers the temperature and concentration gradients. Calculated the effects of nondimensional parameters on velocity, temperature and concentration profile via graph. Ramesh, K. et al.(28) discussed the essential flows of a Casson fluid in flat parallel plates and considered three primary situations such as the plate walls progressing in contradictory directions, the growth of inferior plate in the flow direction and others in a rigid location, the growth of the plates in the flow direction respectively. It was quite interesting to study the behaviour of the fluid in these different scenarios. Shaheen, N. et al.(31) analyzed electrically conducting two-dimensional radiative casson nanofluid flow through a deformable cylinder fixed in a porous medium with the impact of unpredictable characteristics compound with chemical reaction and Arrhenius activation energy. Shankar, S. et al.(32) studied the Casson fluid numerically with MHD through a vertical permeable wall with impacts of triple diffusive on a viscous flow with mixed convection. The fluids nature is examined by the triple diffusive boundary layer stream under the pressure of solutal diffusivity and thermal conductivity. Abbas, N. et al.(1) analyzed unsteady compressible Casson hybrid nanofluid flow over an erect stretching sheet with a stagnation point. Also studied the nonlinear radiation impact in this manner. Gnanaprasanna, K. and Singh, A. K.(5) explained that nanofluid with more shear thinning effects and rheological properties with variable viscosity on a vertical plate using the Prandtl number numerically. Hameed, N. et al.(6) examined the two-dimensional flow of Casson hybrid nanofluid flow on a non-linear extending surface using absorption and heat generation, Magnetic field and viscous dissipation. Irfan, and Khan,(8) examined the two-dimensional magnetohydrodynamic (MHD) casson fluid flow with shear thickening properties for a vertical stretching sheet in the presence of variable heat source and heat transfer characteristics. This paper also considers the velocity slip conditions and the effect of thermal radiation. Jain et al.(10) studied MHD laminar flow with heat, mass, magnetic flux, buoyancy ratio, thermal conduction, radiation, and convective boundary conditions for an electromagnetic fluid. Khashi'ie,

et al.(16) examined how viscous dissipation and MHD affect the transfer of heat radiative of fluid flow of Reiner-Philippoff across a nonlinearly contracting sheet. Lanjwani, et al.(18) studied the two-dimensional steady boundary layer flow, heat transfer, and mass transfer properties of micropolar nanofluids over surfaces that are exponentially expanding and contracting. Mehta et al.(22) studied the magnetohydrodynamics of a convective stagnation point flow with a vertical sheet embedded in a permeable medium. The effects of heat generation/absorption, radiation, and viscous dissipation were all taken into account. Prasad, et al.(26) illustrated the flow of nano-convective magnetohydrodynamic radiation over a cone. Xia, et al. (35) examined the flow of a micropolar hybrid nano-fluid in a 3D nonlinear mixed convective boundary layer under multiple slip conditions and microorganism presence across the thin surface.Jain et al.(11) conducted a study on the spinning fluid flow that occurs when a disk revolves with an inverse linear angular velocity in a magnetic unsteady Brownian motion of viscous nanofluids. Jangid et al.(12) modelled heat and mass transfer in fluid sheets of varying thickness, and stagnant sheets considering heat source/sink, permeability, magnetic fields, radiation, Joule heating, buoyancy force and chemical reactions.The belongings of radiation and velocity slip on MHD stream and melting warmth transmission of a micropolar liquid over an exponentially stretched sheet which is fixed in a porous medium with heat source/sink are accessibled by Kumar et al.(17) Makkar, et al. (20) experimented in the presence of convective conditions and gyrotactic microorganisms with MHD Casson fluid flow and calculated the influence of different fundamental fluid parameters. Reddy, et al. (32) analyzed the MHD casson nanofluid on variable radiative flow with a joule heating effect on a stretching sheet. Sneha, et al.(33) explained two-dimensional MHD incompressible flow which does not depend on time and in this term also calculated the heat transfer of the flow. In the fluid, nanoparticles were added to improve thermal efficiency and also applied a strong transverse magnetic field. As per the authors' conclusion and some research on triple diffusive Casson fluid flow with MHD and convective boundary conditions. Here the motive of this research is to find out the triple diffusive Casson fluid flow with MHD in the existence of radiation and chemical reaction parameters. These studies can also help in developing more accurate and predictive models for various scientific and engineering applications, contributing to advancements in multiple fields. This study helps to find Triple MHD Casson fluid flow with Radiation, source/sink parameter and chemical reaction impacts over a vertical wall with convective boundary conditions. It helps to develop new technologies and experiments. It also has further applications in the fields of security, medicine, engineering, bioscience and industrialized methods such as the refining of waste from plastic, the oil recovery process, polymer extrusion and transpiration cooling process and many more.

2 Problem Structure:

In a two-dimensional MHD Casson mixed convective fluid flow with radiation and joule heating effect, considered temperature T_∞ and free stream velocity U_∞ which is constant over a static porous plane surface. To solve the geometry problem, take the x-axis upwards along with the vertical plate, and the y-axis taken perpendicular to it. Also, consider the velocity components u and v to determine the solution to this problem accurately. [Figure1].
In the solution of two distinguished elements S_n (n=1,2) with concentration, C_n (n=1,2) is assumed. A constant fluid temperature T_f is maintained by the left side of the plate which gives a variable heat transfer h_f. Here ($T_f > T_\infty$) shows the supplementary flow corresponds to the shield being heated by the liquid, and ($T_f < T_\infty$) shows the opposing flow corresponds to the shield being cooled by the fluid.

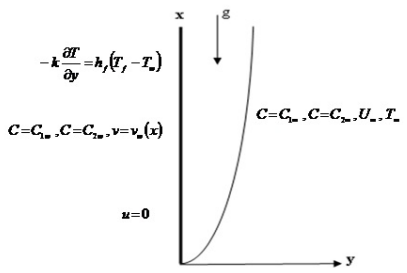

Figure 1: Physical Diagram

The buoyancy approximation is factored in and integrated with the flow region. On the surface, a moving magnetic field $B_0(x)$ is forced. The imposed magnetic field can't be compared to the induced one due to the low magnetic Reynolds number. Above all preliminaries, The fundamental governing PDE's equations are:

$$\frac{\partial u}{\partial x}+\frac{\partial v}{\partial y}=0 \tag{1}$$

$$\begin{aligned} u\frac{\partial u}{\partial x}+v\frac{\partial v}{\partial y} =&\nu(1+\frac{1}{\beta})\frac{\partial^2 u}{\partial y^2}-\frac{\sigma B^2(x)u}{\rho}+g_0[\beta_T(T-T_\infty) \\ &+\beta_{C1}(C_1-C_{1\infty})+\beta_{C1}(C_2-C_{2\infty})] \end{aligned} \tag{2}$$

$$u\frac{\partial T}{\partial x}+v\frac{\partial T}{\partial y}=\alpha\frac{\partial^2 T}{\partial y^2}+\frac{Q_0}{\rho c_p}(T-T_\infty)-\frac{1}{\rho c_p}\frac{\partial q_r}{\partial y} \tag{3}$$

$$u\frac{\partial C_1}{\partial x}+v\frac{\partial C}{\partial y}=D_{B1}\frac{\partial^2 C}{\partial y^2}-R_1(C_1-C_{1\infty}) \tag{4}$$

$$u\frac{\partial C_1}{\partial x}+v\frac{\partial C}{\partial y}=D_{B2}\frac{\partial^2 C}{\partial y^2}-R_2(C_2-C_{2\infty}) \tag{5}$$

The suitable Boundary conditions are:

$$\begin{cases} u=0, v=V_w(x), C_1=C_{1w}, C_2=C_{2w}, -K\frac{\partial T}{\partial y}=h_f(T_f-T_w) & \text{at} \quad y=0 \\ u\to U_\infty, v\to 0, T\to T_\infty, C_1\to C_{1\infty}, C_2\to C_{2\infty} & \text{at} \quad y\to\infty \end{cases} \tag{6}$$

Where, $V_w(x)<0$ and $V_w(x)>0$ represent suction and injection, respectively.

$$\tau_{ij}=\begin{cases} 2(\mu_B+\frac{\tau_y}{\sqrt{2\pi}})e_{ij} & \text{if} \quad \pi>\pi_c \\ 2(\mu_B+\frac{\tau_y}{\sqrt{2\pi}})e_{ij} & \text{if} \quad \pi<\pi_c \end{cases} \tag{7}$$

where τ_{ij} is known as share stress and the yield stress of non-Newtonian fluid is represented by τ_y $\pi=e_{ij}e_{ij}$

Using transformation Similarity in classify to express PDE's(1)-(6) in linear form

$$\begin{cases} u = U_\infty f'(\eta), v = -\frac{1}{2}\sqrt{\frac{U_\infty}{x}}\nu(f(\eta) - \eta f'(\eta)), \eta = y\sqrt{\frac{U_\infty}{(\nu x)}}, \\ \psi = \sqrt{(U_\infty \nu x)} f(\eta), \theta(\eta) = \frac{T - T_\infty}{T_f - T_\infty}, \phi_{1(\eta)} = \frac{C_1 - C_{1\infty}}{C_{1w} - C_{2\infty}}, \phi_{2(\eta)} = \frac{C_2 - C_{2\infty}}{C_{2w} - C_{2\infty}} \end{cases} \tag{8}$$

Where ψ is the stream function and u and v are the velocity components. Reducing the equations (1)-(6) in the form of non-dimensional with the help of equation (8)

$$(1 + \frac{1}{\beta})f''' + \frac{1}{2}ff'' - M^2 f' + \lambda\theta + N_1\phi_1 + N_2\phi_2 = 0 \tag{9}$$

$$(1 + \frac{Nr}{Pr})\theta'' + (\frac{Pr}{2})f\theta' + \lambda_1\theta = 0 \tag{10}$$

$$\phi_1{}'' + \tfrac{1}{2}Sc_1 f\phi_1{}' - R_1 Sc_1\phi_1 = 0 \tag{11}$$

$$\phi_2{}'' + \tfrac{1}{2}Sc_2 f\phi_2{}' - R_2 Sc_2\phi_2 = 0 \tag{12}$$

The boundary conditions are :

$$\begin{cases} f(\eta) = f_w, f'(\eta) = 0, \theta'(\eta) = -a[1 - \theta(\eta)], \phi_1(\eta) = 1, \phi_2(\eta) = 1; & \text{at} \quad \eta = 0 \\ f'(\eta) = 1, \theta(\eta) = 0, \phi_1(\eta) = 0, \phi_2(\eta) = 0; & \text{at} \quad \eta \to \infty \end{cases} \tag{13}$$

where η_∞ is the edge of the boundary layer;

Local Concentration Grashof number$(G_{C1}) = g_0\beta_{C1}(C_1 - C_{1\infty})x^3/\nu^2$
Local Concentration Grashof number$(G_{C2}) = g_0\beta_{C2}(C_2 - C_{2\infty})x^3/\nu^2$
Local Temperature Grashof number$(G_T) = g_0\beta_T(T_f - T_w)x^3/\nu^2$
Prandtl number$(Pr) = \frac{\nu}{\alpha}$
Buoyancy force parameter$(N_1) = \frac{D_{C1}}{{Re_X}^2}$
Buoyancy force parameter$(N_2) = \frac{D_{C2}}{{Re_X}^2}$
Schmidt number$(Sc_1) = \frac{\nu}{D_{B1}}$
Schmidt number$(Sc_2) = \frac{\nu}{D_{B2}}$
Mixed convection Parameter$(\lambda_1) = \frac{G_T}{{Re_X}^2}$
Magnetic parameter$(M) = B_0\sqrt{\frac{\sigma}{\rho U_\infty}}$

When $\lambda_1 > 0$ then the Mixed convection parameter corresponds to assisting flow and when $\lambda_1 < 0$ then it is opposing flow.The coefficient of Skin friction (C_{fx}), the Nusselt number(Nu_x), and the Sherwood numbers (Sh_{x1}),(Sh_{x2}), are defined as,

$$C_{fx} = 2{Re_x}^{-\frac{1}{2}}f''(0), \quad {Re_x}^{-\frac{1}{2}}Nu_x = \theta'(0),$$
$$Sh_{x1} = -{Re_x}^{-\frac{1}{2}}\phi_1{}'(0)), \quad Sh_{x2} = -{Re_x}^{-\frac{1}{2}}\phi_2{}'(0)), \tag{14}$$

3 Results and Discussion:

In this segment, results are calculated with the help of the above equation (9)-(12) and are solved with equation (9) using the BVP4C technique and the outcome are

discussed through graphs. This study numerically calculated the velocity f', temperature θ, concentrations ϕ_1&ϕ_2, skin friction as well as heat transfer for different non-dimensional parameters which are demonstrated in figs (2-18). For the verification of this study, current results are compared to the previous study shown in Table **??** with the Ref. papers (18), (27). The effect of Convective parameter(a) on the profile of velocity. From Fig. 2, It is noticed that if the value of the Convective parameter(a) increased, then the velocity profiles also increased. Also from the boundary condition it is perceived that if 'a' is raised to infinity then the outcomes of surface temperature get a higher value as well. In the profile of velocity, Temperature and concentrations if the suction injection effect is applied, then according to the suction ($f_w > 0$) the fluid is being removed from the flow, which creates a local pressure region in the flow field. elsewhere, in the injection ($f_w < 0$) fluid is added to the flow or the extra fluid is counted. Come to Fig.3 which states the temperature profile, it is easy to understand that when the amount of the fluid is less then the temperature mid between the particle of fluid flow is higher or it is stated that in the impact of suction ($f_w > 0$) creates a lower pressure region in the flow, which can lead to a decrease in temperature due to the decrease in overall energy content of the fluid. This is a result of the reduced enthalpy associated with the lower pressure. The temperature profile near the injection ($f_w < 0$) point can be influenced by the temperature of the injected fluid. If the injected fluid is warmer, it can lead to an increase in temperature in the vicinity of the injection point. The presence of heat sources and sinks can significantly influence fluid flow patterns and temperature distributions within a system. From Fig. 4 and 5, in the presence of the heat source/ sink parameter (λ), the velocity and temperature profile increases when the value of the heat source/sink parameter increases due to variation of thermal energies in the fluid flow. [h]

Table 2: Relative study of Heat Transfer rate at the sheet for numerous ranges of a When f_w= M= $\lambda = 0$ and $Pr = 10$ between Shankar S., et al[27] and the current work.

$constant$	$Ref.(18)$	$Ref.(27)$	$PresentWork$
a	$(-\theta')(0))$	$(-\theta')(0))$	$(-\theta')(0))$
0.8	0.381191	0.381201	0.381186
1	0.421344	0.421252	0.421338
5	0.635583	0.635601	0.635571
10	0.678721	0.678711	0.678707
20	0.702563	0.702601	0.702549

The mixed Convection Parameter (λ_1), inside the Boundary layer wall, increases the velocity as the buoyancy force is added ($\lambda_1 > 0$), the concentration profile decreases when the value of the mixed convection parameter increases which is presented in Fig.6 and Fig.7. The impact of the Magnetic field parameter (M) for the velocity profile is shown in Fig.8 which states that the velocity decreases as the magnetic field is increased. Lorentz force increases as increases the magnetic field, resulting in the resistance increasing as well and due to this the velocity decreases inside the boundary layer. Temperature profile and Concentration profile presented in Fig.9, 10 and 11 give the impact of the Magnetic field (M). The temperature and concentration profiles are observed in the existence of a Magnetic field (M), as the Magnetic field increases in the fluid flow the temperature is increased. The concentration profile also behaves the same as temperature with the magnetic field. Both the Temperature and Concentration profile are increased as increases with the Magnetic field (M). Fig.12 displayed the graph between the temperature profile and Radiation parameter, stating that with the effect of radiation in fluid flow, the

Table 3: Properties of Thermo physical of NaCl and Sucrose at $25°C$ from Shankar S., et al[27].

Components	*Morality*	*Weights%*	$\nu(\times 10^{-}6)$	$D_s(\times 10^{-}6)$	*Sc*	ΔC	*Nc*
	0.01	0.0584	1.003	1.545	649.19	0.0108	-2.48
Nacl	0.05	0.2922	1.007	1.502	670.43	0.03	-6.86
	0.1	0.05844	1.011	1.483	681.72	0.05	-11.43
	0.5	2.922	1.031	1.472	700.4	0.48	-91.51
	1.0	5.844	1.058	1.484	712.93	0.5	-114.3
	0.01	0.342	1.014	0.521	1946.25	0.0108	-1.36
Sucrose	0.05	1.7115	1.043	0.468	2226.4	0.03	-3.77
	0.1	3.423	1.08	0.451	2597.4	0.05	-6.28
	0.5	17.115	1.610	0.442	3635.95	0.4	-50.3
	1.0	34.23	3.535	0.466	7585.83	0.5	-62.87

Table 4: : The rate of coefficient of skin friction, coefficient of transfer of mass, and coefficient of transfer of heat for assorted non-dimensional parameters:

a	f_w	λ	λ_1	N_1	N_2	Nr	β	Pr	M	R_1	R_2	Sc_1	Sc_2	$f"(0)$	$-\theta'(0)$	$-\phi_1{}'(0)$	$-\phi_2{}'(0)$
1														0.941407	0.326776	0.42599	0.456568
2	0.1	0.1	1	1	1.5	0.1	0.5	2	1	0.1	0.1	2.5	3	0.968986	0.393397	0.432001	0.393395
3														0.98079	0.42336	0.434546	0.466287
	-0.2													1.03431	0.256811	0.225586	0.225586
1	-0.1	0.1	1	1	1.5	0.1	0.5	2	1	0.1	0.1	2.5	3	1.0036	0.277131	0.294636	0.294636
	0.1													0.941407	0.326776	0.42599	0.456568
	0.2													0.910529	0.35146	0.500845	0.54919
		0.2												0.955528	0.28894	0.4299	0.460984
1	0.1	0.3	1	1	1.5	0.1	0.5	2	1	0.1	0.1	2.5	3	0.880178	0.37584	0.581348	0.6492
		0.5												1.02367	0.111128	0.448566	0.481968
			2											1.07854	0.336191	0.454996	0.489426
1	0.1	0.1	3	1	1.5	0.1	0.5	2	1	0.1	0.1	2.5	3	1.20887	0.344437	0.480658	0.518284
			4											1.3335	0.351762	0.50368	0.544025
				2										1.4568	0.340277	0.467695	0.503785
1	0.1	0.1	1	2.5	1.5	0.1	0.5	2	1	0.1	0.1	2.5	3	1.24404	0.346181	0.486147	0.52452
				3										1.34026	0.351635	0.50332	0.543742
					2									1.04101	0.33333	0.446169	0.47952
1	0.1	0.1	1	1	2.5	0.1	0.5	2	1	0.1	0.1	2.5	3	1.13785	0.339313	0.46471	0.500502
					3									1.23229	0.344812	0.481884	0.519855
						0.5								0.939397	0.332216	0.425434	0.455939
1	0.1	0.1	1	1	1.5	2.5	0.5	2	1	0.1	0.1	2.5	3	0.934938	0.344333	0.4242	0.454545
						7								0.932304	0.351524	0.423472	0.453721
							1							1.18766	0.337913	0.460554	0.496715
1	0.1	0.1	1	1	1.5	0.1	1.5	2	1	0.1	0.1	2.5	3	1.32315	0.343131	0.476998	0.515822
							2							1.40955	0.346187	0.486713	0.527118
								5						0.890574	0.438856	0.410308	0.438856
1	0.1	0.1	1	1	1.5	0.1	0.5	7	1	0.1	0.1	2.5	3	0.874273	0.487666	0.405927	0.433851
								10						0.858763	0.537411	0.402169	0.429533
									2					0.686251	0.283281	0.293155	0.304612
1	0.1	0.1	1	1	1.5	0.1	0.5	2	2.5	0.1	0.1	2.5	3	0.598314	0.238594	0.238594	0.26554
									3					0.529289	0.182999	0.1943327	0.251155
										0.1				0.965534	0.329515	0.193649	0.466009
1	0.1	0.1	1	1	1.5	0.1	0.5	2	1	0.2	0.1	2.5	3	0.999693	0.333354	0.108434	0.479209
										0.3				0.941407	0.326776	0.42599	0.456568
											0			0.913539	0.323714	0..41661	0.665877
1	0.1	0.1	1	1	1.5	0.1	0.5	2	1	0.1	0.1	2.5	3	0.941407	0.326776	0.42599	0.456568
											0.2			0.978782	0.330841	0.438473	0.199103
												3		0.933673	0.335694	0.452877	0.452877
1	0.1	0.1	1	1	1.5	0.1	0.5	2	1	0.1	0.1	5	3	0.910704	0.322609	0.442281	0.457293
												7		0.895246	0.320677	0.435594	0.62798
													4	0.922117	0.324165	0.417999	0.503224
1	0.1	0.1	1	1	1.5	0.1	0.5	2	1	0.1	0.1	2.5	5	0.906819	0.322148	0.411826	0.545151
													6	0.894242	0.320534	0.406893	0.583771

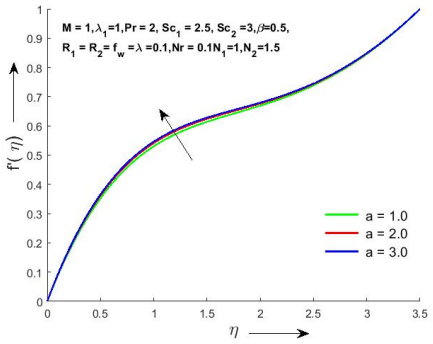

Figure 2: Change in $f'(\eta)$ with assorted values of a(Convective parameter)

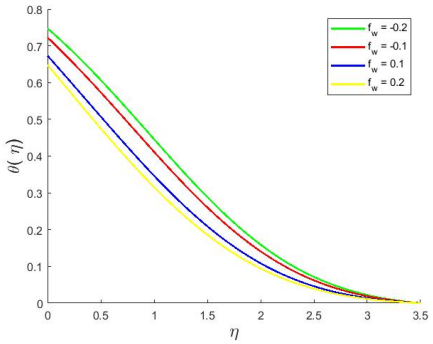

Figure 3: Change in $\theta(\eta)$ with various values of f_w(Injection/Suction Parameter)

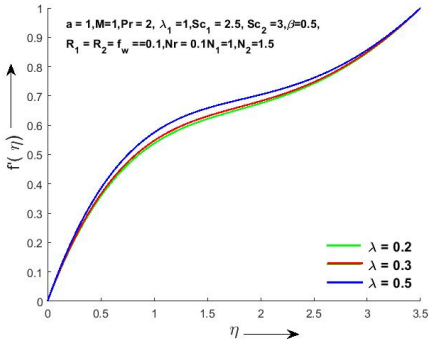

Figure 4: Change in $f'(\eta)$ with assorted values of λ(Heat Source/sink Parameter)

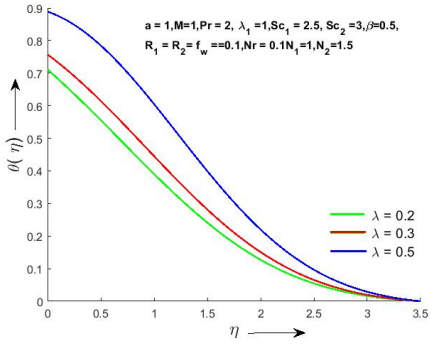

Figure 5: Change in $\theta(\eta)$ with various values of λ(Heat Source/sink Parameter)

temperature decreases. It is noticed that chemical reaction parameters R_1 and R_2 affect the density of fluid flow, which in turn can impact buoyancy forces, pressure gradients, and fluid flow velocity. These changes are particularly relevant in combustion processes, where chemical reactions can release energy and result in changes in temperature, density, and velocity. In Fig.13 to 16 observed that the velocity and concentration profiles increase as R_1 and R_2 increase. Concentration profile ϕ_1 has been taken for R_1, while concentration profile ϕ_2 has been taken for R_2. Based on the earlier study, a higher Schmidt number impacts diffusion and leads to thicker concentration boundary layers, slower mass transport, and potentially different mixing characteristics. Looking at the data presented in Fig.17 and Fig.18, it appears that there are various values of the Schmidt numbers Sc_1 and Sc_1 that impact velocity profiles. Specifically, if the Schmidt number increases, all profiles of velocities decrease.

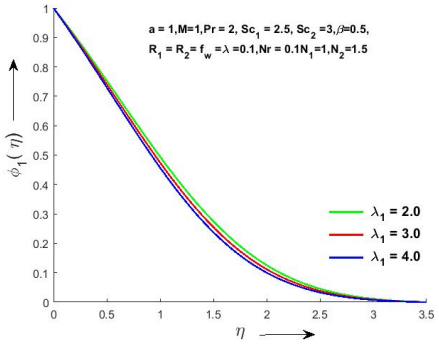

Figure 6: Change in $\phi_1(\eta)$ with assorted values of λ_1(Convection Parameter)

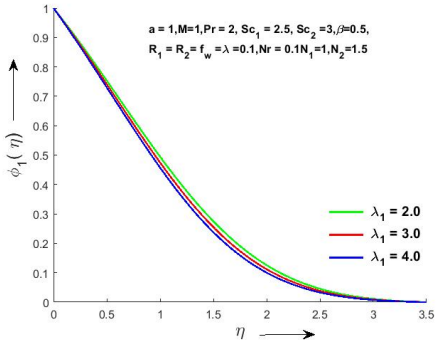

Figure 7: Change in $\phi_1(\eta)$ with assorted values of λ_1(Convection Parameter)

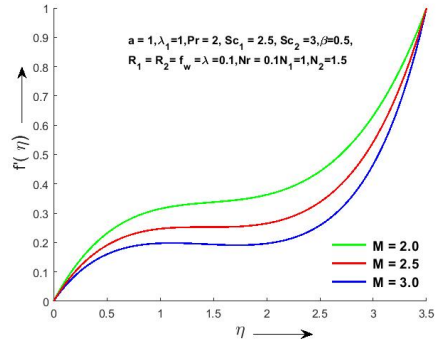

Figure 8: Change in $f'(\eta)$ with assorted values of M(Magnetic Field)

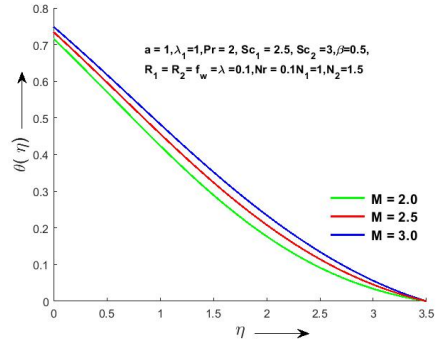

Figure 9: Change in $\theta(\eta)$ with assorted values of M(Magnetic Field)

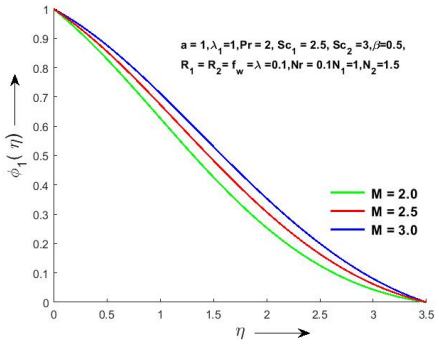

Figure 10: Change in $\phi_1(\eta)$ with assorted values of M(Magnetic Field)

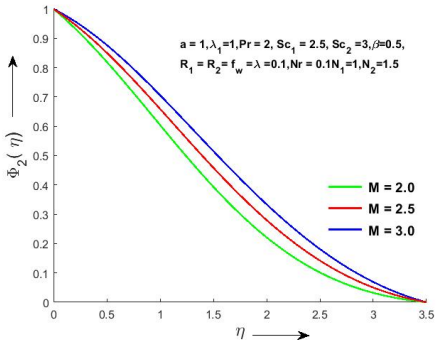

Figure 11: Change in $\phi_2(\eta)$ with assorted values of M(Magnetic Field)

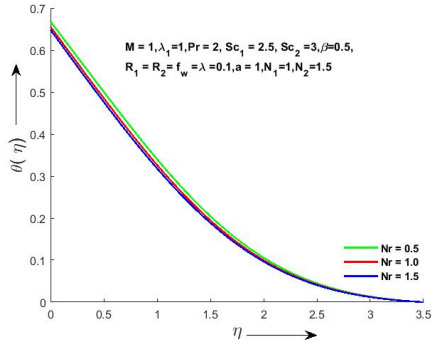

Figure 12: Change in $\theta(\eta)$ with assorted values of Nr(Radiation Parameter)

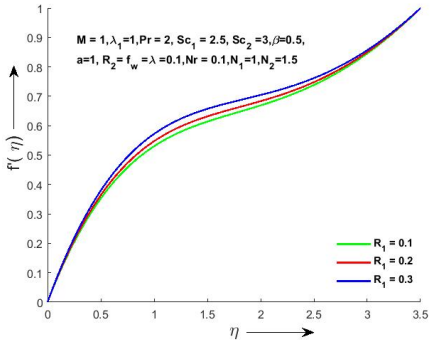

Figure 13: Change in $f'(\eta)$ with assorted values of R_1(Parameter of Chemical Reaction)

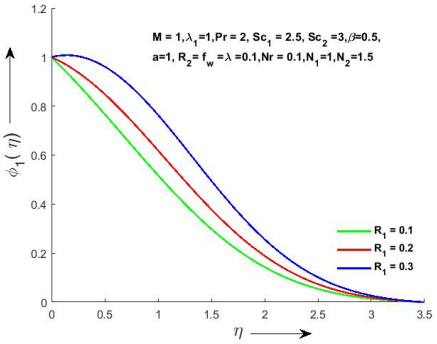

Figure 14: Change in $\phi_1(\eta)$ with assorted values of R_1(Parameter of Chemical Reaction)

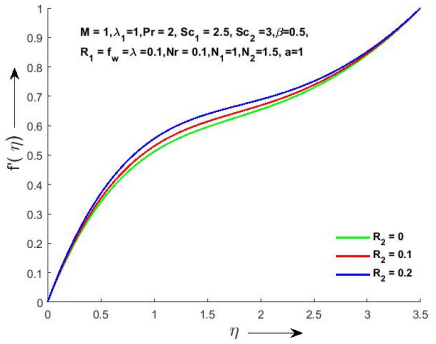

Figure 15: Change in $f'(\eta)$ with assorted values of R_2(Parameter of Chemical Reaction)

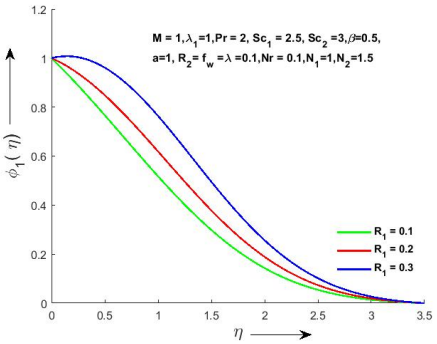

Figure 16: Change in $\phi_1(\eta)$ with assorted values of R_1(Parameter of Chemical Reaction)

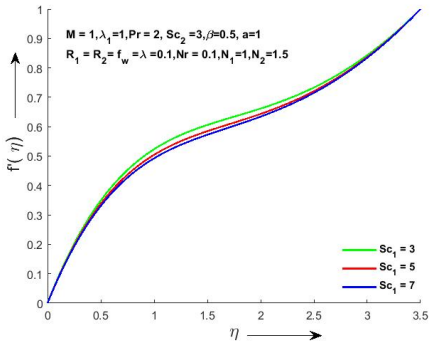

Figure 17: Change in $f'(\eta)$ with assorted values of Sc_1(Schmidt number)

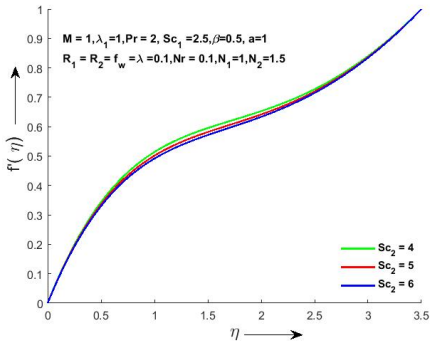

Figure 18: Change in $f'(\eta)$ with assorted values of Sc_2(Schmidt number)

4 Conclusion:

Triple diffusive MHD fluid flow with radiation can lead to valuable insights that can improve technology, resource utilization and our understanding of complex physical phenomena.This numerical study shows that a Casson fluid flows with triple MHD, in the existence of radiation, Chemical reaction and Heat source or sink. The presence of all parameters gets results numerically and graphically, and these are the subsequent results:

- The sucrose concentration boundary layer is thinner than NaCl. Due to the smaller size of NACl ions, the diffusion of NACl particles in the liquid is deeper than that of sucrose.
- The Temperature Profile goes down when Suction/Injection Parameter(f_w) upsurges.
- Boundary layer thickness is upsurged in both velocity and temperature profiles when heat source/sink parameter(λ) enlarges due to variation of thermal energies in the fluid flow,
- When we applied the Magnetic parameter (M), it enhanced the temperature profile and concentration profile but decreased the velocity by raising the value of M.
- The fluid temperature decays when the Radiation parameter (Nr) enlarges.
- The chemical reaction parameters R_1 andR_2 significantly affect the density of fluid flow, the velocity and concentration boost with rising R_1 and R_2.
- The velocity profile increases by the convection parameter 'a' increased.
- In the future, we will extend this flow model to convective heating scenarios including a variety of geometries such as Riga plates, cylindrical sheets, etc.

References

[1] Abbas, N., Shatanawi, W.,& Abodayeh, K. (2022). Computational analysis of MHD nonlinear radiation casson hybrid nanofluid flow at vertical stretching sheet. Symmetry, 14(7), 1494.

[2] Devi, S. S. U., & Devi, S. A. (2016). Numerical investigation of three-dimensional hybrid Cu–Al2O3/water nanofluid flow over a stretching sheet with effecting Lorentz force subject to Newtonian heating. Canadian Journal of Physics, 94(5), 490-496.

[3] Farooq, U., Hussain, M., Ijaz, M. A., Khan, W. A., & Farooq, F. B. (2021). Impact of non-similar modeling on Darcy-Forchheimer-Brinkman model for forced convection of Casson nano-fluid in non-Darcy porous media. International Communications in Heat and Mass Transfer, 125, 105312.

[4] Gireesha, B. J., Archana, M., Prasannakumara, B. C., Gorla, R. R., & Makinde, O. D. (2017). MHD three dimensional double diffusive flow of Casson nanofluid with buoyancy forces and nonlinear thermal radiation over a stretching surface. International Journal of Numerical Methods for Heat & Fluid Flow, 27(12), 2858-2878.

[5] Gnanaprasanna, K., & Singh, A. K. (2022). A numerical approach of forced convection of Casson nanofluid flow over a vertical plate with varying viscosity and thermal conductivity. Heat Transfer, 51(7), 6782-6800.

[6] Hameed, N., Noeiaghdam, S., Khan, W., Pimpunchat, B., Fernandez-Gamiz, U., Khan, M. S., & Rehman, A. (2022). Analytical analysis of the magnetic field, heat generation and absorption, viscous dissipation on couple stress casson hybrid nanofluid over a nonlinear stretching surface. Results in Engineering, 16, 100601.

[7] Hayat, T., Ullah, I., Muhammad, T., & Alsaedi, A. (2017). Radiative three-dimensional flow with Soret and Dufour effects. International Journal of Mechanical Sciences, 133, 829-837.

[8] Irfan, H. M., Khan, A. (2022). Numerical Investigation of Suction/Injuction on Triple Diffusive MHD Casson Fluid Flow over a Vertical Stretching Surface. International Journal of Advancements in Mathematics, 2(2), 105-122.

[9] Isa, S. S. P. M., Arifin, N. M., Nazar, R., Bachok, N., Ali, F. M., & Pop, I. (2017). MHD mixed convection boundary layer flow of a Casson fluid bounded by permeable shrinking sheet with exponential variation. Scientia Iranica, 24(2), 637-647.

[10] Jain, R., Mehta, R., Rathore, H., Singh, J. (2022). Analysis of Soret and Dufour Effect on MHD Fluid Flow Over a Slanted Stretching Sheet with Chemical Reaction, Heat Source and Radiation. In Advances in Mathematical Modelling, Applied Analysis and Computation: Proceedings of ICMMAAC 2021 (pp. 571-597). Singapore: Springer Nature Singapore.

[11] Jain, R., Mehta, R., Mehta, T., Singh, J., Baleanu, D. (2023). MHD flow and heat and mass transport investigation over a decelerating disk with ohmic heating and diffusive effect. Thermal Science, 27(Spec. issue 1), 141-149.

[12] Jangid, S., Mehta, R., Singh, J., Baleanu, D., Alshomrani, A. S. (2023). Heat and mass transport of hydromagnetic Williamson nanofluid passing through a permeable media across an extended sheet of varying thickness. Thermal Science, 27(Spec. issue 1), 129-140.

[13] Jena, S., Dash, G. C., & Mishra, S. R. (2018). Chemical reaction effect on MHD viscoelastic fluid flow over a vertical stretching sheet with heat source/sink. Ain Shams Engineering Journal, 9(4), 1205-1213.

[14] Khan, Z.H.; Khan, W.A.; Sheremet, M.A.(2020). Enhancement of heat and mass transfer rates through various porous cavities for triple convective-diffusive free convection. Energy, 201, https://doi.org/10.1016/j.energy.2020.117702.

[15] Khan, Z.H.; Khan, W.A.; Tang, J.; Sheremet, M.A. (2020). Entropy generation analysis of triple diffusive flow past a horizontal plate in porous medium. Chemical Engineering Science,228,https://doi.org/10.1016/j.ces.2020.115980.

[16] Khashi'ie, N. S., Waini, I., Kasim, A. R. M., Zainal, N. A., Ishak, A., & Pop, I. (2022). Magnetohydrodynamic and viscous dissipation effects on radiative heat transfer of non-Newtonian fluid flow past a nonlinearly shrinking sheet: Reiner–Philippoff model. Alexandria Engineering Journal, 61(10), 7605-7617.

[17] Kumar, R., Singh, J., Mehta, R., Kumar, D.,& Baleanu, D. (2023). Analysis of the impact of thermal radiation and velocity slip on the melting of magnetic hydrodynamic micropolar fluid-flow over an exponentially stretching sheet. Thermal Science, 27(Spec. issue 1), 311-322.

[18] Lanjwani, H. B., Chandio, M. S., Anwar, M. I., Al-Johani, A. S., Khan, I., & Alam, M. (2022). Triple Solutions with Stability Analysis of MHD Mixed Convection Flow of Micropolar Nanofluid with Radiation Effect. Journal of Nanomaterials, 2022.

[19] Lund, L. A., Omar, Z., Khan, I., Raza, J., Sherif, E. S. M., & Seikh, A. H. (2020). Magnetohydrodynamic (MHD) flow of micropolar fluid with effects of viscous dissipation and joule heating over an exponential shrinking sheet: triple solutions and stability analysis. Symmetry, 12(1), 142.

[20] Makkar, V., Poply, V., & Sharma, N. (2023). Three-dimensional magnetohydrodynamic non-Newtonian bioconvective nanofluid flow influenced by gyrotactic microorganisms over stretching sheet. Heat Transfer,vol 52,issue1 pg.548-562.

[21] Manjappa, A.; Jayanna, G.B.; Chandrappa, P.B. (2019). Triple diffusive flow of Casson nanofluid with buoyancy forces and non-linear thermal radiation over a horizontal plate. Archives of Thermodynamics, 40, 49-69,https://doi.org/10.24425/ather.2019.12828.

[22] Mehta, R., Kumar, R., Rathore, H., Singh, J. (2022). Joule heating effect on radiating MHD mixed convection stagnation point flow along vertical stretching sheet embedded in a permeable medium and heat generation/absorption. Heat Transfer, 51(8), 7369-7386.

[23] Nawaz, M.; Awais, M. (2020). Triple diffusion of species in fluid regime using tangent hyperbolic rheology. Journal of Thermal Analysis and Calorimetry, https://doi.org/10.1007/s10973-020-10026-0.

[24] Parvin, S., Balakrishnan, N., & Isa, S. S. P. M. (2021). MHD Casson fluid flow under the temperature and concentration gradients. Magnetohydrodynamics (0024-998X), 57(3).

[25] Patil, P.M.; Roy, M.; Roy, S.; Momoniat, E. (2018). Triple diffusive mixed convection along a vertically moving surface. International Journal of Heat and Mass Transfer, 117, 287-295, https://doi.org/10.1016/j.ijheatmasstransfer.2017.09.106.

[26] Prasad, J. R., Rao, I. V., Balamurugan, K. S., & Dharmaiah, G. (2022). Radiative Magnetohydrodynamic Flow Over a Vertical Cone Filled With Convective Nanofluid. Communications in Mathematics and Applications, 13(2), 449.

[27] Raghunatha, K.R.; Shivakumara, I.S.; Shankar, B.M. (2018). Weakly nonlinear stability analysis of triple diffusive convection in a Maxwell fluid saturated porous layer. Applied Mathematics and Mechanics, 39, 153-168, https://doi.org/10.1007/s10483-018-2298-6.

[28] Ramesh, K., Riaz, A., & Dar, Z. A. (2021). Simultaneous effects of MHD and Joule heating on the fundamental flows of a Casson liquid with slip boundaries. Propulsion and Power Research, 10(2), 118-129.

[29] Rao, P. S., Prakash, O., Mishra, S. R., & Sharma, R. P. (2020). Similarity solution of three-dimensional MHD radiative Casson nanofluid motion over a stretching surface with chemical and diffusion-thermo effects. Heat Transfer, 49(4), 1842-1862.

[30] Reddy, B. N., & Maddileti, P. (2023). Casson nanofluid and joule parameter effects on variable radiative flow of MHD stretching sheet. Partial Differential Equations in Applied Mathematics, 100487.

[31] Shaheen, N., Alshehri, H. M., Ramzan, M., Shah, Z., & Kumam, P. (2021). Soret and Dufour effects on a Casson nanofluid flow past a deformable cylinder with variable characteristics and Arrhenius activation energy. Scientific Reports, 11(1), 19282.

[32] Shankar, S., Ramakrishna, S. R., Gullapalli, N., & Samuel, N. (2021). Triple diffusive MHD Casson fluid flow over a vertical wall with convective boundary conditions. Biointerface Res Appl Chem, 11, 13765-13778.

[33] Sneha, K. N., Bognar, G., Mahabaleshwar, U. S., Singh, D. K., & Singh, O. P. (2023). Magnetohydrodynamics Effect of Marangoni Nano Boundary Layer Flow And Heat Transfer With CNT And Radiation. Journal of Magnetism and Magnetic Materials, 170721.

[34] Umavathi, J.C.; Ali, H.M.; Patil, S.L. (2020). Triple diffusive mixed convection flow in a duct using convective boundary conditions. Mathematical Methods in the Applied Sciences, 43, 9223-9244, https://doi.org/10.1002/mma.6617.

[35] Xia, W. F., Ahmad, S., Khan, M. N., Ahmad, H., Rehman, A., Baili, J., & Gia, T. N. (2022). Heat and mass transfer analysis of nonlinear mixed convective hybrid nanofluid flow with multiple slip boundary conditions. Case Studies in Thermal Engineering, 32, 101893.